Optimization of Ultrasmall Superparamagnetic Iron Oxide (P904)-enhanced Magnetic Resonance Imaging of Lymph Nodes: Initial Experience in a Mouse Model

ROH-EUL YOO[1*], HYE RIM CHO[1,2*], SEUNG HONG CHOI[1,3,4], JAE-KYUNG WON[5], JI-HOON KIM[1] and CHUL-HO SOHN[1]

Departments of [1]Radiology, [2]Radiation Applied Life Science, and [5]Pathology, Seoul National University College of Medicine, Seoul, Republic of Korea; [3]Center for Nanoparticle Research, Institute for Basic Science, and [4]School of Chemical and Biological Engineering, Seoul National University, Seoul, Republic of Korea

Abstract. *Background: P904 is a novel ultra-small superparamagnetic iron oxide (USPIO) contrast agent. This study was conducted to investigate the optimal dose of P904 for magnetic resonance imaging (MRI) of lymph nodes. Materials and Methods: T2*-weighted 3T MRI was performed in 14 normal mice before and 24 h after P904 injection at varying doses. Normalized signal intensity (nSI), signal-to-noise ratio (SNR), contrast-to-noise ratio (CNR), and contrast ratio (CR) were calculated to determine the optimal dose. MRI of the metastatic lymph node models (n=5) was acquired using the optimal dose and correlated with pathological results to calculate sensitivity and specificity. The mean SI ratio between pre- and postcontrast MRI was also calculated for each lymph node. Results: The mean nSI and SNR values on postcontrast images were significantly lower at 300 μmol Fe/kg than at 75 μmol Fe/kg (p<0.001). The mean CNR and CR values were significantly higher at 300 μmol Fe/kg than at the other two doses (p<0.05). At the optimal dose of 300 μmol Fe/kg, the mean SI ratio of benign lymph nodes was significantly lower than that of metastatic lymph nodes (p<0.001). The Az (areas under the receiver operating characteristic curves) value for diagnosing lymph node metastasis at the optimal dose was 0.97. Conclusion: The optimal dose for P904-enhanced MRI of the lymph nodes was 300 μmol Fe/kg, which could be used for the diagnosis of lymph node metastasis.*

*These authors contributed equally to this study.

Correspondence to: Seung Hong Choi, MD, Ph.D., Department of Radiology, Seoul National University College of Medicine, 28, Yongon-dong, Chongno-gu, Seoul, 110-744, Korea. Tel: +82 220722861, Fax: +82 27477418, e-mail: verocay@snuh.org

Key Words: Animal study, lymph node metastasis, magnetic resonance imaging of lymph nodes, MRI, P904, ultra-small superparamagnetic iron oxide particle, USPIO.

P904 (Guerbet Laboratories, Paris, France) is a novel ultra-small superparamagnetic iron oxide (USPIO) contrast agent, which has been shown to have a shorter blood half-life and a higher *in vitro* macrophage uptake when compared with ferumoxtran-10 (Combidex; Advanced Magnetics, Cambridge, MA, USA; also known as Sinerem, AMI-7227, AMI-227, and BMS 180549), the most widely evaluated first-generation USPIO particle (1).

The majority of the previous studies on P904 have focused on its capability to depict vascular inflammation as in atherosclerotic plaque imaging (2-5). In addition to risk stratification for plaque rupture, its potential role in monitoring efficacy of therapeutic interventions such as anti-inflammatory drugs has been investigated and has shown some encouraging results.

Apart from plaque imaging, magnetic resonance imaging (MRI) of lymph nodes has been another major subject of interest in terms of clinical applications for USPIO particles. The need for development of a tissue-specific, highly sensitive and specific imaging technique to facilitate nodal characterization has become apparent from past studies, which revealed limitations of various parameters – nodal morphology, border, signal intensity (SI) characteristics, enhancement kinetics, apparent diffusion coefficient, and ^{18}F-fluorodeoxyglucose (^{18}F-FDG) and ^{18}F-choline uptake – in diagnosing small metastatic or hyperplastic benign nodes (6-14). Some promising results regarding the diagnosis of lymph node metastasis have been reported for USPIO particles, particularly ferumoxtran-10; nonetheless, it has not yet succeeded in receiving final Food and Drug Administration (FDA) approval (15). More recently, the feasibility of diagnosing lymph node metastasis with P904

was investigated in a preliminary experimental study, in which P904 yielded higher sensitivity and specificity in discriminating benign from metastatic lymph nodes, with higher signal differences between benign and metastatic lymph nodes, compared with ferumoxtran-10 (1). The optimal dose for P904-enhanced MRI of lymph nodes, however, was not fully evaluated in the preliminary study.

The aim of this experimental study using BALB/c nude mice was to evaluate the optimal dose of P904 for contrast-enhanced MRI of the lymph nodes. Concepts of contrast-to-noise ratio (CNR) and contrast ratio (CR), as well as the normalized signal intensity (nSI) and signal to-noise ratio (SNR), were adopted to reflect conspicuity of the signal drop due to T2* effect of the USPIO particle at different P904 doses (16). In addition, the optimal dose of P904 was used to depict lymph node metastases.

Materials and Methods

This experiment was approved by the Animal Care Committee at our institution (IACUC 10-0235).

Animal preparation. The experiment was performed using 19 6-week-old BALB/c nude mice (ORIENT, Sungnam, Kyunggi, Korea). The animals were allowed food and water *ad libitum*. Fourteen normal BALB/c nude mice were used to determine the optimal dose of P904 that produces the maximum T2* effect in normal lymph nodes. Murine B16F10 melanoma cells (American Type Culture Collection [ATCC], Rockville, MD, USA), with high potential to metastasize to regional lymph nodes, were implanted into the bilateral upper brachial areas of the remaining five mice to create an animal model of metastatic lymph nodes, following a previously-reported method (17). From the American Type Culture Collection (ATCC, Rockville, MD, USA), the B16F10 cells were obtained and maintained in Dulbecco's modified Eagle's medium with 10% fetal bovine serum at 37˚C (17). For the metastatic lymph node models, MRI was performed with a 3.0T scanner one week after cell implantation.

MRI contrast material. P904, a new USPIO particle for macrophage imaging, was used in this study. P904 consists of a maghemite core and a coating of a low-molecular-weight amino-alcohol derivative of glucose, which is equivalent to 2000 hydroxyl groups per nanoparticle (4). P904 has a hydrodynamic diameter of approximately 21 nm, which is slightly smaller than that of ferumoxtran-10 (*i.e.* 30 nm) (1). With regard to T1 and T2 relaxivities, r1 and r2 of P904 measured in water at 1.42 T and 37˚C were 14 and 87 mM^{-1} s^{-1} , respectively (4).

MRI. Prior to MRI, the mice were anesthetized by intraperitoneal injection of a solution containing zolazepam (5 mg/kg, Zoletil®; Virbac, Carros cedex, France) and xylazine (10 mg/kg, Rompun®; Bayer-Schering Pharma, Leverkusen, Germany). All MRI were performed using a 3.0 T scanner (TrioTim; Siemens, Erlangen, Germany) with a 4-channel wrist coil.

Optimization of P904 dose for lymph node imaging in normal mice. At day one, a precontrast coronal T2*-weighted three-dimensional (3D) gradient-echo sequence was acquired after routine localization images. P904 was prepared in the following three different doses to find the optimal dose for lymph node imaging: 300, 150, and 75 μmol Fe/kg. Normal BALB/c nude mice (n=14) were divided into three groups and P904 was administered to the mice of each group *via* their tail veins: 300 μmol Fe/kg (n=5), 150 μmol Fe/kg (n=4), and 75 μmol Fe/kg (n=5). A postcontrast coronal T2*-weighted 3D gradient-echo sequence was acquired 24 hours after the contrast administration. The scans covered the entire region from the neck to the upper thigh.

The imaging parameters, including repetition time, echo time, number of signals acquired, and section thickness, were modified to find the optimized values for accurate depiction of the brachial and inguinal lymph nodes. The optimized parameters thus selected were as follows: repetition time/echo time, 40 ms/22 ms; flip angle, 12º; field of view, 49×70 mm; matrix, 256×180; slice thickness, 0.6 mm; number of excitations, 6; and pixel resolution, 0.2×0.4×0.6 mm.

Metastatic lymph node model. As for the five mice of the metastatic lymph node model, the optimal dose determined using the normal mice was administered *via* their tail veins. Pre- and postcontrast coronal T2*-weighted 3D gradient-echo images were acquired using the same parameters.

Isolation of lymph nodes and histopathological examination. After the acquisition of the postcontrast T2*-weighted MR images, all five metastatic lymph node models were sacrificed, and their brachial and inguinal lymph nodes were isolated by one author (H.R.C.). The lymph nodes were fixed with 10% formalin and embedded in paraffin. Afterwards, the lymph nodes were sectioned at 0.5-mm intervals, and from each 0.5-mm section, a 4-μm-thick slide was prepared for hematoxylin-eosin (H&E) staining and subsequently examined by a pathologist (J.K.W.) for the presence of metastasis.

Image analysis. The MRI data were digitally transferred from a picture archiving and communication systems (PACS) workstation to a personal computer and processed with Image J (available at http://rsb.info.nih.gov/ij/) and software developed in-house using Microsoft Visual C++.

Qualitative analysis for differentiation of benign and metastatic lymph nodes in metastatic lymph node models: Two investigators (S.H.C. and J.H.K. with seven and 15 years of experience in the interpretation of MRI studies), who were blinded to the histopathologic information, performed the qualitative analysis of the MRIs presented in random order by one author (R.E.Y.). All the MRIs were reviewed on a PACS workstation. A diagnosis of malignancy was made by consensus, using previously reported criteria (13, 18, 19): a lymph node with an overall high SI, an eccentric or central high SI with darkening along its peripheral rim on the postcontrast T2*-weighted MRI was considered to be malignant. On the other hand, a node with an overall dark SI, an overall dark SI apart from its fatty hilum, an overall dark SI with tiny speckles of high SI, or a central low SI on the postcontrast T2*-weighted MRI was considered to be nonmalignant.

Quantitative analysis of the SI of each lymph node: Quantitative analysis of the SI for each lymph node was performed by one author (R.E.Y.). On each section of the T2*-weighted MRIs, a region of interest (ROI) was drawn to include the entire area of a brachial or an inguinal lymph node using Image-J software. The data acquired from each section were summated to derive voxel-by-voxel SIs for

the entire lymph node by using software developed in-house. Given the earlier findings that the muscle tissue remains unchanged by the contrast agent (18, 19), the voxel-by-voxel SI values of the lymph node were normalized with respect to the SI of the shoulder muscle, which was measured using a single ROI of 3-5 mm^2, to cancel the SI fluctuations related to variations in technical parameters between the pre- and postcontrast images. The following formula was used to calculate the SI ratio from the nSIs: SI ratio=$(SI_{lymph\ node[post-P904]}/SI_{muscle[post-P904]})/(SI_{lymph\ node[pre-P904]}/SI_{muscle[pre-P904]})$. Furthermore, SNR, CNR, and CR were calculated using the following equations (20-23):

$SNR = SI_{lymph\ nodes} / \sigma_{noise\ (air)}$

$CNR = | SI_{lymph\ nodes} - SI_{muscle} | / \sigma_{noise\ (air)}$

$CR = | SI_{lymph\ nodes} - SI_{muscle} | / | SI_{lymph\ nodes} + SI_{muscle} |$

where $SI_{lymph\ nodes}$ is the average signal intensity of the brachial or inguinal lymph nodes, $\sigma_{noise(air)}$ is the standard deviation of the background noise measured at the air with a ROI of 3-5 mm^2, and SI_{muscle} is the average signal intensity of the shoulder muscle.

Statistical analysis. Statistical analyses were performed using commercially available software (MedCalc, version 8.0.0.1; MedCalc software, Mariakerke, Belgium). The data for each parameter was assessed for normality with the Kolmogorov-Smirnov test. In all tests, *p*-values less than 0.05 were considered statistically significant.

Optimization of P904 dose for lymph node imaging in normal mice. For each group to which a different dose of P904 was administered [300 μmol Fe/kg (n=5), 150 μmol Fe/kg (n=4), and 75 μmol Fe/kg (n=5)], the paired Student *t*-test was used to assess whether there was a significant difference in the mean nSI, SNR, CNR, and CR values of the brachial and inguinal lymph nodes between the pre- and postcontrast images.

To determine the optimal dose of P904, the pre- and postcontrast mean nSI, SNR, CNR, and CR values of the lymph nodes of the three groups were compared, using repeated measurements analysis of variance (ANOVA) with Tukey–Kramer post hoc comparisons for multiple comparisons.

Metastatic lymph node model. Qualitative analysis for differentiation of benign and metastatic lymph nodes: Sensitivity and specificity for differentiation of the benign and metastatic lymph nodes were calculated for mice of the metastatic lymph node model (n=5) to which the optimal dose of P904 was administered. Data clustering (*i.e.* more than one lesion per mouse) was accounted for with the method reported by Rao and Scott (24).

Metastatic lymph node model. Quantitative analysis of the SI in each lymph node: With respect to the optimal P904 dose, Mann–Whitney *U*-test was used to assess whether the mean SI ratio of the benign lymph nodes differed significantly from that of the metastatic lymph nodes.

Receiver operating characteristic (ROC) curve analysis was performed to determine the optimal cutoff value of the mean SI ratio, which provided a balance between sensitivity and specificity for the diagnosis of lymph node metastasis. The Az value (areas under the receiver operating characteristic curves) as well as the corresponding sensitivity and specificity at the optimal cutoff value were calculated, along with 95% confidence intervals (CIs).

Table I. *Changes in the mean magnetic resonance imaging parameters of the normal brachial and inguinal lymph nodes after P904 administration*.

	Precontrast MRI	Postcontrast MRI	*p*-Value
300 μmol Fe/kg P904 (n=20)			
nSI	1.58±0.60	0.33±0.14	<0.001
SNR	46.73±19.30	9.55±2.84	<0.001
CNR	16.19±15.54	22.19±11.39	0.172
CR	0.19±0.17	0.51±0.15	<0.001
150 μmol Fe/kg P904 (n=16)			
nSI	1.44±0.46	0.58±0.25	<0.001
SNR	47.08±17.11	16.21±7.22	<0.001
CNR	15.81±13.08	13.32±5.92	0.494
CR	0.18±0.13	0.31±0.15	0.015
75 μmol Fe/kg (n=20)			
nSI	1.83±0.50	1.10±0.46	<0.001
SNR	44.72±22.84	30.42±17.06	0.031
CNR	21.27±15.96	8.89±8.46	0.004
CR	0.27±0.13	0.17±0.11	0.010

Values are the mean±standard deviation. Data in parentheses are the number of lymph nodes. *p*-Values were calculated with the paired Student *t*-test. nSI: normalized signal intensity, SI of the lymph node normalized to that of the shoulder muscle; SNR: signal-to- noise ratio, calculated by SNR: $SI_{lymph\ nodes} / \sigma_{noise\ (air)}$; CNR: contrast-to-noise ratio, calculated by $| SI_{lymph\ nodes} - SI_{muscle} | / \sigma_{noise\ (air)}$; CR: contrast ratio, calculated by $| SI_{lymph\ nodes} - SI_{muscle} | / | SI_{lymph\ nodes} + SI_{muscle} |$, where SIlymph nodes is the average signal intensity of the brachial or inguinal lymph nodes, $\sigma_{noise\ (air)}$ is the standard deviation of the background noise measured in air, and SImuscle is the average signal intensity of the shoulder muscle.

Results

Optimization of P904 dose for lymph node imaging in normal mice. The mean nSI, SNR, CNR, and CR values of the normal brachial and inguinal lymph nodes before and after P904 administration are summarized in Table I for each P904 dose. The mean nSI and SNR values of the postcontrast images were significantly lower than those of the precontrast images at all three P904 doses. However, the postcontrast mean CNR value was higher than the precontrast mean CNR value only at the dose of 300 μmol Fe/kg, without statistical significance. As for the CR, the mean values were significantly higher in the postcontrast images than in the precontrast images at both 300 μmol Fe/kg and 150 μmol Fe/kg of P904.

In terms of the SIs on precontrast MRIs, no significant differences were found in the mean nSI, SNR, CNR, and CR values of the lymph nodes for all three P904 concentrations ($p>0.05$). After P904 administration, however, the mean nSI and SNR values were significantly lower at the P904 dose of 300 μmol Fe/kg than at 75 μmol Fe/kg ($p<0.001$). The mean nSI and SNR values at the dose of 300 μmol Fe/kg were also

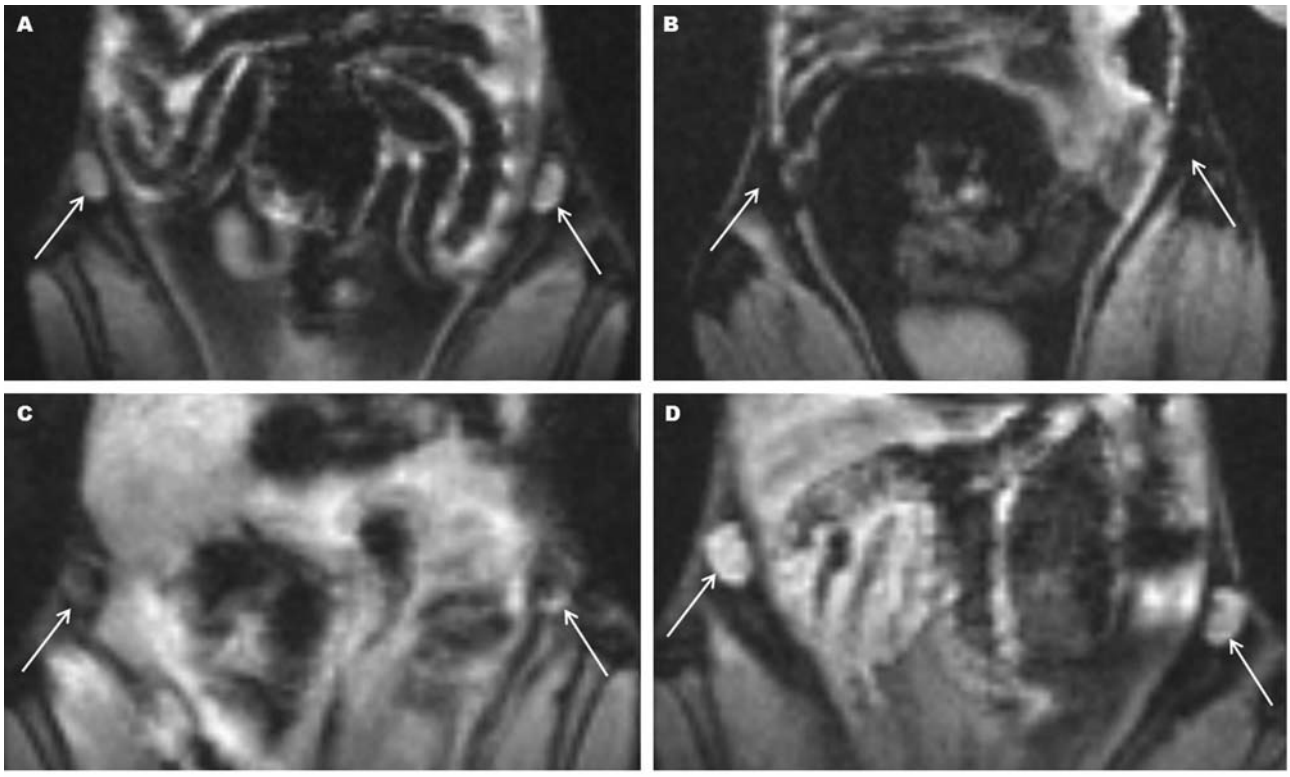

Figure 1. *Coronal T2*-weighted magnetic resonance images of normal inguinal lymph nodes of 6-week old BALB/c nude mice before (A: arrows) and after P904 administration (B, C, D: arrows) at different doses (B: 300 μmol Fe/kg; C: 150 μmol Fe/kg; and D: 75 μmol Fe/kg). Signal drop due to T2* effect of the particle is most evident at the dose of 300 μmol Fe/kg (B: arrows).*

lower than those at the dose of 150 μmol Fe/kg, although these differences did not reach statistical significance ($p>0.05$). Concordantly, the mean CNR value at the P904 dose of 300 μmol Fe/kg was significantly higher than those at the other two P904 doses ($p<0.05$ and $p<0.001$ when compared with 150 μmol Fe/kg and 75 μmol Fe/kg, respectively). The mean CR value was also significantly higher at the dose of 300 μmol Fe/kg than at the lower doses of P904 ($p<0.001$ when compared with 150 μmol Fe/kg and 75 μmol Fe/kg) (Table II). Representative cases for each P904 dose are provided in Figure 1.

According to the results presented in Tables I and II and Figure 1, the concentration of 300 μmol Fe/kg was determined to be the optimal dose of P904 for lymph node imaging.

Metastatic lymph node model. Qualitative analysis for differentiation of benign and metastatic lymph nodes: Owing to the high metastatic potential of murine B16F10 melanoma cells and the method of implantation, metastasis was produced exclusively in all brachial lymph nodes (n=10) and not in inguinal lymph nodes (n=10), resulting in a sensitivity of 100% (10 out of 10) (95% CI=56-100%) and a specificity of 100% (10 out of 10) (95% CI=56-100%) for differentiating benign from metastatic lymph nodes in the qualitative analysis. Figure 2 illustrates the typical benign and metastatic lymph nodes depicted with the optimal dose.

Metastatic lymph node model. Quantitative analysis of the SI in each lymph node: The mean SI ratio of the benign lymph nodes was significantly lower than that of the metastatic lymph nodes at the optimal dose of 300 μmol Fe/kg: 0.27±0.11 *vs*. 0.77±0.42, respectively ($p<0.001$).

The optimal cut-off value for the mean SI ratio at the optimal dose was 0.314, with the corresponding sensitivity and specificity being 100% (95% CI=69-100%) and 80% (95% CI=44-98%), respectively. The Az value was 0.97 (95% CI=0.78-1.00).

Discussion

The present study evaluated the optimal dose for P904-enhanced MRI of lymph nodes, and for this purpose, we analyzed the nSI, SNR, CNR, and CR at each administered dose. Finally, the optimal dose of P904 (300 μmol Fe/kg) was used to depict lymph node metastases. The P904 dose of 300 μmol Fe/kg demonstrated significantly higher mean

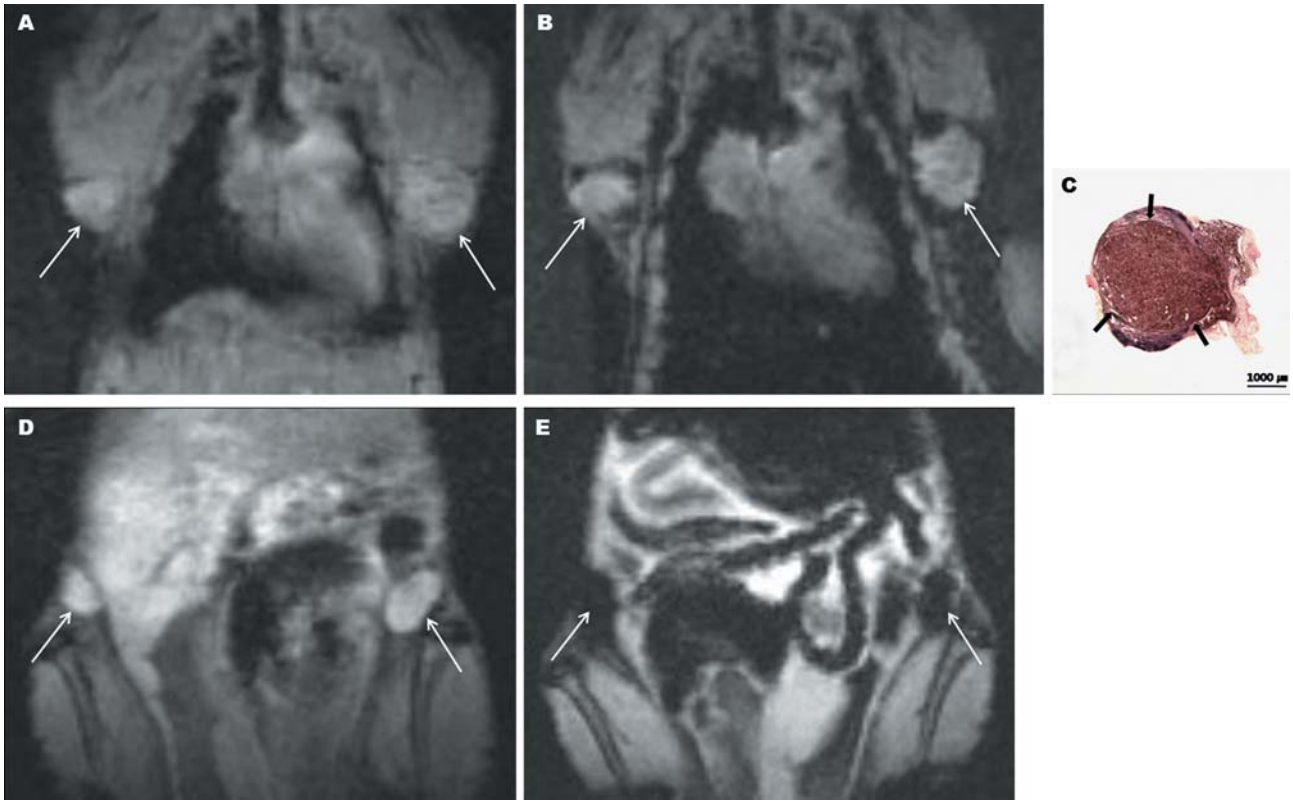

Figure 2. *A metastatic lymph node model (6-week old BALB/c nude mice) into which 300 μmol Fe/kg of P904 was administered. Signal intensities of the metastatic brachial lymph nodes (A, B: arrows) remain mostly unchanged on the postcontrast coronal T2*-weighted magnetic resonance image (B), compared with the precontrast image (A), except at the periphery. The hematoxylin-eosin-stained pathology specimen (C) of the right brachial lymph node at low-power field (magnification, ×12.5) well-demonstrates a large metastatic focus (arrows). In contrast, the benign inguinal lymph nodes (D, E: arrows) show overall dark signal intensities on the postcontrast image (E), compared with the precontrast image (D).*

CNR and CR values compared with the doses of 150 μmol Fe/kg and 75 μmol Fe/kg. The mean nSI and SNR values at the dose of 300 μmol Fe/kg were also lower than those at the other two doses, although the differences did not reach statistical significance in comparisons with the dose of 150 μmol Fe/kg. Hence, the optimal dose for P904-enhanced MRI of lymph nodes was determined to be 300 μmol Fe/kg, and metastatic foci were clearly evident on postcontrast T2*-weighted MRIs at the optimal dose. With regard to quantitative analysis of the SI, the mean SI ratio of the benign lymph nodes was significantly lower than that of the metastatic lymph nodes ($p<0.001$), yielding an Az value of 0.97 for diagnosing lymph node metastasis.

P904 is a recently developed USPIO particle for macrophage imaging. Macrophages, a major component of the mononuclear phagocyte system, play a pivotal role in inflammation *via* antigen presentation, phagocytosis, and immunomodulation through production of various cytokines and growth factors (25). Particularly, their contributions to plaque formation and provocation of instability and rupture have been highlighted in previous studies on atherosclerosis, stimulating interest in the development of non-invasive imaging techniques to visualize macrophage burden and to monitor plaque activity as well as the efficacy of therapeutic interventions (2). Accordingly, P904 was first such agent investigated in the context of atherosclerosis for its ability to detect plaque inflammation (2-5). Specifically, Sigovan *et al*. demonstrated that P904 enabled earlier detection of plaque inflammation than ferumoxtran-10 because of its faster blood pharmacokinetics and its early uptake in the reticuloendothelial system (4). In a further study on the use of P904 for treatment monitoring in a mouse model of atherosclerosis, P904 enabled detection of a treatment-related reduction in the macrophage content of atherosclerotic plaques (5).

Meanwhile, lymph node imaging, a leading application field for USPIO particles, has been relatively underexplored for P904. USPIO-enhanced MRI is believed to enable the detection of metastatic foci within lymph nodes regardless of the lymph node size, by T2* effect of the iron oxide particles phagocytosed by functional macrophages, which

Table II. *Postcontrast mean nSI, SNR, CNR, and CR values of the normal brachial and inguinal lymph nodes at different P904 doses.*

	Postcontrast MRI	*p*-Value*	*p*-Value**
300 μmol Fe/kg P904 (n=20)			
nSI	0.33±0.14	NA	>0.05
SNR	9.55±2.84	NA	>0.05
CNR	22.19±11.39	NA	<0.05
CR	0.51±0.15	NA	<0.001
150 μmol Fe/kg P904 (n=16)			
nSI	0.58±0.25	>0.05	NA
SNR	16.21±7.22	>0.05	NA
CNR	13.32±5.92	<0.05	NA
CR	0.31±0.15	<0.001	NA
75 μmol Fe/kg (n=20)			
nSI	1.10±0.46	<0.001	<0.001
SNR	30.42±17.06	<0.001	<0.001
CNR	8.89±8.46	<0.001	>0.05
CR	0.17±0.11	<0.001	<0.05

Values are the mean±standard deviation. Data in parentheses are the number of lymph nodes. *p*-Values were calculated using the repeated measurements analysis of variance (ANOVA) with Tukey–Kramer post hoc comparisons for multiple comparisons with the values at the P904 doses of 300 (*) and 150 (**) μmol Fe/kg, respectively. nSI: normalized signal intensity, SI of the lymph node normalized to that of the shoulder muscle; SNR: signal-to- noise ratio, calculated by $SI_{lymph\ nodes}/\sigma_{noise\ (air)}$; CNR: contrast-to-noise ratio, calculated by $|SI_{lymph\ nodes} - SI_{muscle}|/\sigma_{noise\ (air)}$; CR: contrast ratio, calculated by $|SI_{lymph\ nodes} - SImuscle|/|SI_{lymph\ nodes} + SI_{muscle}|$, where $SI_{lymph\ nodes}$ is the average signal intensity of the brachial or inguinal lymph nodes, $\sigma_{noise\ (air)}$ is the standard deviation of the background noise measured in air, and SI_{muscle} is the average signal intensity of the shoulder muscle; NA: not available.

cause the signal drop of non-metastatic lymph nodes on USPIO-enhanced MRIs. In contrast, the SIs of the metastatic lymph nodes lacking functional macrophages are known to remain unchanged (26, 27). In a preliminary experimental study by Kinner *et al*. (1), P904 was shown to have higher sensitivity and specificity for diagnosing lymph node metastasis in rabbits than ferumoxtran-10 (75% and 100% *vs*. 67% and 94%, respectively), with greater differences in signal (SNR) change over time between benign and metastatic lymph nodes.

Given the positive results of the preliminary study, a question regarding the optimal dose of P904-enhanced MRI of lymph nodes has been raised by the authors. The P904 dose used in the preliminary study by Kinner *et al*. was 200 μmol Fe/kg body weight (1). However, a recommended dose of P904 has not yet been established for the MRI of lymph nodes, calling for an appropriate dose range study. In our preliminary study using normal BALB/c nude mice, the CNR and CR were calculated in addition to the nSI and SNR for a more meticulous evaluation of conspicuity of the signal drop due to the T2* effect of the iron oxide particles. Concepts of CNR and CR have been employed in previous studies on the utility of high b-value diffusion-weighted MRI (DWI) in the evaluation of hyperacute or acute ischemic strokes (16, 23). Kim *et al*. (23) speculated that enhanced lesion conspicuity at a high b-value was attributed to an increased CNR between the lesion and normal brain parenchyma. In another study by Cihangiroglu *et al*. (16), better lesion conspicuity at the high b-value, despite lower SNR and CNR values, was conceived to be related to a higher CR value. In our dose range study incorporating the concepts of CNR and CR as well as nSI and SNR, the mean nSI and SNR values were lower at the dose of 300 μmol Fe/kg than at the dose of 150 μmol Fe/kg, but these differences did not achieve statistical significance. However, the mean CNR and CR values at the P904 dose of 300 μmol Fe/kg were significantly higher than those at the dose of 150 μmol Fe/kg, accounting for the most conspicuous signal drop on the postcontrast images at the dose of 300 μmol Fe/kg.

At the optimal dose of 300 μmol Fe/kg, the mean SI ratio of the benign lymph nodes was significantly lower than that of the metastatic lymph nodes ($p<0.001$), with the optimal cutoff value of 0.314 yielding a sensitivity of 100%, a specificity of 80%, and an Az value of 0.97. Along with the aforementioned results of the preliminary study by Kinner *et al*. (1), our results imply that P904 could be a potentially useful agent for contrast-enhanced MRI of lymph nodes in the oncological field, where the presence or absence of lymph node metastases heavily influences therapeutic decision making.

There were a few limitations to the current study. First of all, the sensitivity and specificity for diagnosing lymph node metastasis in our qualitative analysis were likely to have been inflated because the metastatic foci were produced exclusively in brachial lymph nodes, potentially influencing the two investigators' diagnostic judgments on the presence of metastasis. Second, although histopathology was used as a gold standard in the qualitative analysis, quantitative correlation between the SIs and the tumor burdens of metastatic lymph nodes could not be conducted for the following two reasons: i) sample size was relatively small to establish statistical significance; and ii) most of the metastatic foci created in the mice of the metastatic lymph node model were large in size, resulting in a limited size range. Further study using a larger sample size with heterogeneity in sizes of the metastatic foci would be warranted for accurate quantitative correlation of the SI with histopathology. Third, our MRI protocol did not include T1- and T2-weighted images, which are known to enhance the visualization of anatomy including the fatty hilum (28). Nevertheless, it is widely appreciated from previous studies that pre- and postcontrast T2*-weighted 3D gradient-echo sequences are

the key sequences for demonstrating USPIO particle uptake in lymph nodes (29). Furthermore, the imaging parameters in our study were optimized so that the acquisition of the T2*-weighted gradient-echo sequences alone would be adequate for delineation of the relevant anatomy.

In conclusion, the optimal dose for P904-enhanced MRI of lymph nodes was determined to be 300 μmol Fe/kg in our preliminary experimental study using a mouse model. Diagnostic performance for predicting lymph node metastasis was high at the optimal dose, implying that P904 may be a potentially useful agent for the MRI of lymph nodes in the oncological field.

Acknowledgements

This study was supported by a grant from the National R&D Program for Cancer Control, Ministry of Health & Welfare, Republic of Korea (1120300), the Korea Healthcare technology R&D Projects, Ministry for Health, Welfare & Family Affairs (A112028 and HI13C0015) and by the Research Center Program of IBS (Institute for Basic Science) in Korea.

References

1 Kinner S, Maderwald S, Albert J, Parohl N, Corot C, Robert P, Baba HA and Barkhausen J: Comparison of two different iron oxide-based contrast agents for discrimination of benign and malignant lymph nodes. Invest Radiol *47*: 511-515, 2012.

2 Millon A, Dickson SD, Klink A, Izquierdo-Garcia D, Bini J, Lancelot E, Ballet S, Robert P, Mateo de Castro J, Corot C and Fayad ZA: Monitoring plaque inflammation in atherosclerotic rabbits with an iron oxide (P904) and (18)F-FDG using a combined PET/MR scanner. Atherosclerosis *228*: 339-345, 2013.

3 Sigovan M, Bessaad A, Alsaid H, Lancelot E, Corot C, Neyran B, Provost N, Majd Z, Breisse M and Canet-Soulas E: Assessment of age-modulated vascular inflammation in *ApoE*$^{-/-}$ mice by USPIO-enhanced magnetic resonance imaging. Invest Radiol *45*: 702-707, 2012.

4 Sigovan M, Boussel L, Sulaiman A, Sappey-Marinier D, Alsaid H, Desbleds-Mansard C, Ibarrola D, Gamondès D, Corot C, Lancelot E, Raynaud JS, Vives V, Laclédère C, Violas X, Douek PC and Canet-Soulas E: Rapid-clearance iron nanoparticles for inflammation imaging of atherosclerotic plaque: initial experience in animal model. Radiology *252*: 401-409, 2009.

5 Sigovan M, Kaye E, Lancelot E, Corot C, Provost N, Majd Z, Breisse M and Canet-Soulas E: Anti-inflammatory drug evaluation in *ApoE*$^{-/-}$ mice by ultrasmall superparamagnetic iron oxide-enhanced magnetic resonance imaging. Invest Radiol *47*: 546-552, 2012.

6 Antoch G, Stattaus J, Nemat AT, Marnitz S, Beyer T, Kuehl H, Bockisch A, Debatin JF and Freudenberg LS: Non-small cell lung cancer: dual-modality PET/CT in preoperative staging. Radiology *229*: 526-533, 2003.

7 Brown G, Richards CJ, Bourne MW, Newcombe RG, Radcliffe AG, Dallimore NS and Williams GT: Morphologic predictors of lymph node status in rectal cancer with use of high-spatial-resolution MR imaging with histopathologic comparison. Radiology *227*: 371-377, 2003.

8 Choi EK, Kim JK, Choi HJ, Park SH, Park BW, Kim N, Kim JS, Im KC, Cho G and Cho KS: Node-by-node correlation between MR and PET/CT in patients with uterine cervical cancer: diffusion-weighted imaging versus size-based criteria on T2WI. Eur Radiol *19*: 2024-2032, 2009.

9 Dwamena BA, Sonnad SS, Angobaldo JO and Wahl RL: Metastases from non-small cell lung cancer: mediastinal staging in the 1990s–meta-analytic comparison of PET and CT. Radiology *213*: 530-536, 1999.

10 Fischbein NJ, Noworolski SM, Henry RG, Kaplan MJ, Dillon WP and Nelson SJ: Assessment of metastatic cervical adenopathy using dynamic contrast-enhanced MR imaging. Am J Neuroradiol *24*: 301-311, 2003.

11 Kim JH, Beets GL, Kim MJ, Kessels AG and Beets-Tan RG: High-resolution MR imaging for nodal staging in rectal cancer: are there any criteria in addition to the size? Eur J Radiol *52*: 78-83, 2004.

12 Kitajima K, Murphy RC and Nathan MA: Choline PET/CT for imaging prostate cancer: an update. Ann Nucl Med *27*: 581-591, 2013.

13 Pieterman RM, van Putten JW, Meuzelaar JJ, Mooyaart EL, Vaalburg W, Koëter GH, Fidler V, Pruim J and Groen HJ: Preoperative staging of non-small-cell lung cancer with positron-emission tomography. N Engl J Med *343*: 254-261, 2000.

14 Vesselle H, Pugsley JM, Vallières E and Wood DE: The impact of fluorodeoxyglucose F 18 positron-emission tomography on the surgical staging of non-small cell lung cancer. J Thorac Cardiovasc Surg *124*: 511-519, 2002.

15 Wu L, Cao Y, Liao C, Huang J and Gao F: Diagnostic performance of USPIO-enhanced MRI for lymph-node metastases in different body regions: A meta-analysis. Eur J Radiol *80*: 582-589, 2011.

16 Cihangiroglu M, Citci B, Kilickesmez O, Firat Z, Karlıkaya G, Uluğ AM, Bingol CA and Kovanlikaya I: The utility of high b-value DWI in evaluation of ischemic stroke at 3T. Eur J Radiol *78*: 75-81, 2011.

17 Choi SH, Cho HR, Kim HS, Kim YH, Kang KW, Kim H and Moon WK: Imaging and quantification of metastatic melanoma cells in lymph nodes with a ferritin MR reporter in living mice. NMR Biomed *25*: 737-745, 2012.

18 Weissleder R, Stark DD, Engelstad BL, Bacon BR, Compton CC, White DL, Jacobs P and Lewis J: Superparamagnetic iron oxide: pharmacokinetics and toxicity. AJR Am J Roentgenol *152*: 167-173, 1989.

19 Hauger O, Delalande C, Deminière C, Fouqueray B, Ohayon C, Garcia S, Trillaud H, Combe C and Grenier N: Nephrotoxic nephritis and obstructive nephropathy: evaluation with MR imaging enhanced with ultrasmall superparamagnetic iron oxide-preliminary findings in a rat model. Radiology *217*: 819-826, 2000.

20 Chenevert TL, Sundgren PC and Ross BD: Diffusion imaging: insight to cell status and cytoarchitecture. Neuroimaging Clin N Am *16*: 619-632, 2006.

21 Cihangiroglu M, Uluğ AM, Firat Z, Bayram A, Kovanlikaya A and Kovanlikaya I: High b-value diffusion-weighted MR imaging of normal brain at 3T. Eur J Radiol *69*: 454-458, 2009.

22 González RG, Schaefer PW, Buonanno FS, Schwamm LH, Budzik RF, Rordorf G, Wang B, Sorensen AG and Koroshetz WJ: Diffusion-weighted MR imaging: diagnostic accuracy in patients imaged within 6 hours of stroke symptom onset. Radiology *210*: 155-162, 1999.

23 Kim HJ, Choi CG, Lee DH, Lee JH, Kim SJ and Suh DC: High-b-value diffusion-weighted MR imaging of hyperacute ischemic stroke at 1.5T. AJNR Am J Neuroradiol *26*: 208-215, 2005.
24 Rao JN and Scott AJ: A simple method for the analysis of clustered binary data. Biometrics *48*: 577-585, 1992.
25 Fujiwara N and Kobayashi K: Macrophages in inflammation. Curr Drug Targets Inflamm Allergy *4*: 281-286, 2005.
26 Misselwitz B: MR contrast agents in lymph node imaging. Eur J Radiol *58*: 375-382, 2006.
27 Narayanan P, Iyngkaran T, Sohaib SA, Reznek RH and Rockall AG: Pearls and pitfalls of MR lymphography in gynecologic malignancy. Radiographics *29*: 1057-1069, 2009.
28 Islam T and Harisinghani MG: Overview of nanoparticle use in cancer imaging. Cancer Biomark *5*: 61-67, 2009.
29 Harisinghani MG, Dixon WT, Saksena MA, Brachtel E, Blezek DJ, Dhawale PJ, Torabi M and Hahn PF: MR lymphangiography: imaging strategies to optimize the imaging of lymph nodes with ferumoxtran-10. Radiographics *24*: 867-878, 2004.

Received June 1, 2014
Revised July 11, 2014
Accepted July 14, 2014